

# Oleate prevents palmitate-induced mitochondrial dysfunction in chondrocytes

**Maria Vaquez-Mosquera**

INIBIC

**Mercedes Fernandez-Moreno**

INIBIC

**Estefania Cortes-Pereira**

INIBIC

**Sara Relaño**

INIBIC

**Andrea Dalmao-Fernandez**

INIBIC

**Alejandro Duran-Sotuela**

INIBIC

**Paloma Ramos-Louro**

INIBIC

**Ignacio Rego Pérez**

INIBIC

**Francisco J Blanco** (✉ [fblagar@sergas.es](mailto:fblagar@sergas.es))

UNIVERSIDAD DE A CORUÑA <https://orcid.org/0000-0001-9821-7635>

---

## Research article

**Keywords:** Osteoarthritis; chondrocytes; mitochondrial function; fatty acids; lipid droplets.

**Posted Date:** January 17th, 2020

**DOI:** <https://doi.org/10.21203/rs.2.21189/v1>

**License:**  This work is licensed under a Creative Commons Attribution 4.0 International License.

[Read Full License](#)

---

# Abstract

**BACKGROUND :** The clear association between obesity and osteoarthritis (OA) in joints not subjected to mechanical overload, together with the relationship between OA and metabolic syndrome (MS), suggests that there are systemic factors related to metabolic disorders that are involved in the metabolic phenotype of OA. The aim of this work is to study the effects of palmitate (PA) and oleate (OL), as the most abundant fatty acids (FA) present in the diet and serum, on cellular metabolism in an "in vitro" model of human chondrocytes. **METHODS :** The Seahorse XF96 Analyzer was used to measure the mitochondrial, glycolytic function and the contribution of the mitochondrial oxidative phosphorylation system (OXPHOS) and glycolysis to the production of ATP, in the T/C-28a2 chondrocyte treated with PA, OL and palmitate/oleate (PA/OL) ratio 1:2. Subsequently ATP bioluminescence assay kit was used for ATP quantification. To detect the presence of lipid droplets, two types of stains were performed and the amount of Triglycerides was quantified spectrophotometrically. **RESULTS :** PA, but not OL, produces mitochondrial dysfunction observed with a lower rate of OCR intended for the synthesis of ATP, coupling efficiency, maximal respiration and spare respiratory capacity. Glycolytic function showed lower rates for both glycolytic capacity and glycolytic reserve when cells were incubated with FA in relation to basal condition (BC). The production rate of ATP from OXPHOS showed lower values in chondrocytes incubated with any of the FAs. The evaluation of possible formation of Lipid droplets (LD) showed a significant increase of these structures in FA conditions, being significantly higher when the cells were incubated with OL. **CONCLUSIONS :** PA and OL show antagonistic effects in human chondrocytes; while increased levels of PA induce mitochondrial dysfunction and hinder the response of chondrocytes through the glycolytic pathway, OL shows a cytoprotective effect through which promotes the formation of triglycerides-rich LD, as well as the incorporation of PA.

## Background

Osteoarthritis (OA) is a chronic progressive disorder that first manifests as a molecular derangement (abnormal tissue metabolism), followed by anatomical and/or physiological derangements characterized by cartilage degradation, bone remodeling, osteophyte formation, joint inflammation and loss of normal joint function that can culminate in illness (1).

New insights into the pathophysiology of OA have produced a division of the disease into different clinical and structural phenotypes, whose definition allows specific treatments (2). However, Mechanisms of metabolic OA remain unknown. Obesity is one of the most known OA-associated risk factors, mainly explained as an effect of joint overload. However, (i) the close association of other metabolic diseases such as insulin resistance, dyslipidemia and hypertension, and OA (3–5); (ii) a higher prevalence of OA in non-obese subjects with a metabolically abnormal phenotype in relation to obese subjects without associated metabolic disease (6); and (iii) the positive interaction between obesity and OA in joints not subject to overload, such as OA of hands (7); suggest that systemic factors related to metabolic disorders are involved in this OA subgroup. An increase in plasma fatty acids (FA) is one of the systemic factors related to the different metabolic pathologies (8,9). The most abundant FA present in the diet and blood

are palmitic acid (PA), a long-chain saturated FA, and oleic acid (OL), a monounsaturated FA (8). Synovial fluid, a plasma ultrafiltrate, provides nutrients necessary for the maintenance of articular cartilage. This fluid contains more FA in OA patients than in healthy subjects (10). The effects of FA in tissues have been reported to differ according to the type of FA. Saturated FA, such as PA, have been described to have highly lipotoxic effects, producing apoptosis in different cell types (11–13). The lipotoxic effects of PA have also been studied for monounsaturated FA, such as OL, showing in most cases that OL reverses these effects (14–16).

Given the limited oxygen availability conditions of articular cartilage, chondrocytes are well adapted to maintain their extracellular matrix synthesis function with minimal nutrient input and low oxygen consumption; this is the reason why these cells mainly use the glycolytic pathway to obtain energy. However, the ATP obtained from mitochondrial respiration is known to significantly contribute to the synthesis of collagen and proteoglycans of the extracellular matrix of articular cartilage (17). Mitochondrial dysfunction, which has been reported in human OA chondrocytes, may affect several pathways that have been implicated in cartilage degradation, including oxidative stress, inflammation, cartilage matrix calcification and chondrocyte apoptosis (18,19).

Considering that (i) synovial fluid from OA patients has more FA and that these FA are more lipotoxic than those in healthy subjects (10), and even that (ii) accumulated FA have been detected in OA cartilage OA (20), in this study we used an *in vitro* model of human chondrocytes, to characterize the effects of the two major FA in blood and in the diet (PA and OL) on cellular metabolism.

## Methods

**Cell Culture and Treatment** The T/C-28a2 chondrocyte cell line (HSS Research Institute, New York, NY, USA) was maintained in Dulbecco's Modified Eagle Medium (DMEM) (Gibco, Grand Island, NY, USA), supplemented with 10% fetal bovine serum (FBS; Gibco), penicillin (100 U/ml)/streptomycin (100 µg/ml) (Gibco). PA, OL and PA/OL in a ratio of 1:2 stock solutions were prepared at 5 mM in 10% bovine serum albumin (BSA; Sigma Aldrich, St.Louis, MO,USA), as a vehicle for PA 200 mM and OL 700 mM (Sigma Aldrich) solutions. These solutions were incubated at 55° for 30 minutes (21). Then, for each condition of FA, the different test concentration solutions were prepared in DMEM without FBS. For the baseline condition (BC), DMEM without FBS was used, to which the corresponding BSA percentage was added. The experiments were performed after 12h of incubation with the FA.

### Cell viability assay

Cell viability after the exposure to various concentrations of PA, OL and PA/OL mix (0.4, 0.7, and 1mM) was assessed using the MTS assay (Promega). The incubation medium with tested compounds (12 hours) was changed to a medium with the MTS reagent at the end of exposure and cells were incubated for additional 3 h at 37°C. The absorbance of dissolved formazan was measured at 490 nm in a microplate reader. Data are displayed as a percentage of cells with basal condition (BC).

## Quantification of superoxide anion(O<sub>2</sub><sup>-</sup>) production

To measure superoxide anion (O<sub>2</sub><sup>-</sup>) production, cells were incubated with 4 µg/µl Mitosox™ in Hank's Buffered Salt Solution (HBSS) (Thermo Fisher Scientific, Waltham, MA, USA) for 15 minutes at 37°C and 5% CO<sub>2</sub> in darkness. The pelleted cells were re-suspended to measure fluorescence by flow cytometry (Becton Dickinson, Franklin Lakes, NJ, USA).

## Quantitative Real-Time PCR

Real-time PCR was performed with a LightCycler 480-II Instrument (Roche Diagnostics, [Risch-Rotkreuz, Suiza](#)) with TaqManUniversal Master Mix (Roche). Gene expression was calculated relative to the housekeeping gene (*RPL13A*). Sequence primers, probes and PCRconditions are shown in Additional file 1.Table S1.

## Extracellular Flux Analysis

The Seahorse XFpExtracellular Flux Analyzer (Agilent Technologies, Santa Clara, CA, USA) was used to estimate the chondrocyte metabolic stress. Based on the presence of sensors sensitive to the concentration of oxygen and protons, this technique allows to measure simultaneously, in living cells, the two main cellular energy pathways:mitochondrial respiration and glycolysis.

### 1. Mitochondrial stress testing

2x10<sup>4</sup> cells were seeded in XFp Cell Culture Miniplates (Agilent Technologies). Following incubation with the FA, the assay was carried out following the manufacturer's recommendations. The oxygen consumption rate (OCR) was determined in the presence of specific mitochondrial modulators successively added: 2mM oligomycin (OLG); 1mM carbonyl cyanide-p-trifluoromethoxyphenylhydrazine (FCCP); and finally a mixture of rotetone and antimycin A (Rot/AntA) 0.5mM. Each condition was performed in triplicate and the data obtained (normalized by cell number) was used to calculate the Basal respiration, ATP synthesis, Proton leak, Maximal respiration, Spare respiratory capacity, and the Non-mitochondrial respiration, expressed as OCR (pmol/min)/10<sup>3</sup> cells; and Coupling efficiency as a percentage (Additional file 2.Table S2a).

### 2. Glycolysis stress testing

2x10<sup>4</sup> cells were seeded in XFp Cell Culture Miniplates.Following incubation with the FA, the cells were incubated in medium without glucose or pyruvate and the extracellular acidification rate (ECAR) was measured. Then, the different modulators were separately injected: 10mM glucose, 2µM OLG and 50mM 2-deoxyglucose (2-DG). Each condition was performed in triplicate and the data obtained in the test was used to calculate the Glycolysis rate and the Glycolytic capacity, expressed as ECAR (mpH/min)/10<sup>3</sup>cells; and Glycolytic reserve expressed as a percentage (Additional file 2.Table S2b).

## Assessment of energy balance

### Contribution of mitochondrial oxidative phosphorylation system (OXPHOS) and glycolysis to the production of ATP

Taking into account that, under normal conditions, the stoichiometry ratio of OCR and proton production rate (PPR) with the ATP production is 5 and 1 respectively (22), from the OCR and PPR data obtained from the Seahorse XFp Extracellular Flux Analyzer, the rate of ATP production (pmol / min) due to OXPHOS and glycolysis was estimated.

### Quantification of total and mitochondrial ATP by luminescence

To measure intracellular ATP, an ATP bioluminescence assay kit (Roche Applied Science) was used according to the manufacturer's recommendations. T/C-28a2 chondrocytes were treated with FA before incubation for two hours with a solution of 156mM NaCl, 3mM KCl, 2mM MgSO<sub>4</sub>, 1.25mM KH<sub>2</sub>PO<sub>4</sub>, 2mM CaCl<sub>2</sub> dihydrate, 20mM HEPES and 10mM glucose for the quantification of total ATP; or 5mM 2-DG and 5mM of sodium pyruvate for the quantification of mitochondrial ATP. The ATP levels were normalized to the protein concentration.

## Mitochondrial DNA (mtDNA) copy number quantification

To confirm the level of mitochondrial DNA recovered after incubation with FA, the mtDNA copy number was determined by real time polymerase chain reaction as previously described (23). The targeted genes were the mitochondrial 12S ribosomal gene (forward 5'-CCACGGGAAACAGCAGTGAT-3', reverse 5'-CTATTGACTTGGGTAAATCGTGTGA-3') and RNaseP (forward: 5'-GCACTGAGCACGTTGAGAGA-3'; reverse: 5'-CCAGTCGAAGAGCTCCAGA-3'). For determining mtDNA copy number, an independent standard curve was generated for each gene (12S-rRNA and RNaseP). The total mtDNA copy number was determined from the Ct values and was extrapolated into the external standard curve. The concentration for each gene was obtained in the analyzed samples. MtDNA copy number values were expressed by the ratio 12S rRNA/RNaseP. To normalize the values between all experiments, we established the mtDNA copy number using the BC condition as 100%.

## Evaluation of lipid accumulation

10<sup>4</sup> cells were seeded in each well of a chamber slide (Thermo Fisher Scientific) and incubated with the different FA conditions described above. After fixation for 10 minutes with a 4 % paraformaldehyde solution, the following two stains were applied:

OilRed-O (1- [2,5-dimethyl-4- (2,5-dimethylphenylazo) phenylazo] -2-naphthol) staining: for 20 minutes, then counter stained with haematoxylin. The proportion of positively stained cells was analyzed and quantified using *Image J*, "Image Processing and Analysis in Java," software (National Institutes of Health, Bethesda, MD, USA)

LD540 (4,4-Difluoro-2,3,5,6-bis-tetramethylene-4-bora-3a, 4a-diaza-indacene) staining: for 30 minutes at a 1:10,000 dilution, then counter stained with Hoechst 33258 solution (Sigma Aldrich). To quantify positivity of LD540 staining were analyzed by flow cytometry (Becton Dickinson).

### **Quantification of intracellular triglycerides**

Following 12 h culture of T/C-28a2 cells with the different FA conditions, the cells were collected to determine their triglyceride content. A suspension of the intracellular content of the cells was obtained by sonication. The samples were then centrifuged at 10,000xg for 10 min at 4°C. For the spectrophotometric quantification of triglycerides (TG) the Glycerol Phosphate Oxidase / Peroxidase method was used (Biosystems, Barcelona, Spain), following the manufacturer's instructions.

### **Statistical analysis**

Appropriate statistical analyses were performed using GraphPad Prism v6 software. Differences between the mean of the groups were determined using unpaired and nonparametric t-test. The results are reported as mean  $\pm$  SD. A p value less than 0.05 was considered significant.

## **Results**

### **Cell viability assay**

The effects of different FA concentrations on the chondrocyte cell line T/C-28a2 were evaluated with the CellTiter 96® Aqueous Non-Radioactive Cell Proliferation Kit Assay. The values obtained for each condition (n=3) were normalized in relation to the basal condition (BC) to which a value of 100% was assigned. There are no significant differences between the viability of the cells in the basal condition and that of the cells exposed to different concentrations of PA, OL and PA / OL: 0.4 mM, 0.7 mM and 1 mM (Figure 1). From the results obtained in this assay and taking into account the physiological range values of the plasma/serum FA (24,25), we chose 0.7 mM as the concentration to perform the subsequent analyses proposed in this work.

### **Palmitate induces mitochondrial dysfunction and increased production of superoxide anion in chondrocytes**

Globally, the OCR values showed a lower rate of oxygen consumption when the cells were incubated with PA (vs. BC). The OCR value was slightly recovered under OL and PA/OL conditions, but was always lower than in the basal condition. A lower response to modulators of mitochondrial respiration in cells grown in the presence of PA than that found in the rest of the conditions was also observed. To assess mitochondrial function more accurately, different parameters that were calculated from the OCR data shown in Figure 2 are explained and analyzed in detail as follows:

Cells incubated with FA showed a lower **basal respiration** (Figure 2b) than those in the basal condition, being statistically significant only after incubation with PA (p=0.034). The OCR corresponding to **ATP**

**synthesis** (Figure 2c), **coupling efficiency** (Figure 2d) and **maximum mitochondrial respiration** (Figure 2e) was significantly lower in cells incubated with PA ( $p=0.015$ ,  $0.001$  and  $0.030$  respectively). In contrast, no significant differences in relation to the basal condition were found for cells incubated with OL and the PA/OL 1:2 ratio (Figs. 2b-e).

Regarding the **spare respiratory capacity** (Figure 2f), cells incubated with PA showed significantly lower OCR values than the basal condition ( $p=0.04$ ), whilst cells incubated with OL showed higher OCR levels in relation to the basal condition, although did not reach the statistical significance ( $p=0.053$ ).

The OCR due to **proton leak** (Figure 2g) was significantly higher in cells treated with PA in relation, not only to the basal condition ( $p=0.017$ ), but also when compared with OL ( $p=0.004$ ) and the PA/OL 1:2 ratio ( $p=0.005$ ).

To analyze whether the differences described above could be due to differences in mitochondrial content, the number of mtDNA copies was quantified. As shown in Figure 2h, no significant differences in this parameter were detected. Regarding the levels of **mitochondrial superoxide anion** ( $O_2^-$ ), these were significantly higher after PA incubation ( $p=0.002$ ), while no significant difference was detected after PA:OL 1:2 ratio incubation, when compared with basal condition (Figure 2i).

### **Analysis of glycolytic function by measurement of the extracellular acidification rate (ECAR)**

To evaluate the main parameters of glycolytic after incubation with the different FA, ECAR data obtained in the Seahorse XFP Extracellular Flux Analyzer after stimulation with glucose, OLG and 2-DG, represented in Figure 3a, were analyzed.

The ECAR analysis showed important differences in each condition in relation to the basal condition, with those related to the injection of OLG showing the most notable differences (Figure 3a). To define and assess the meaning of the ECAR data, different parameters were calculated. Compared to the basal condition, a slight, but not significant, decrease in the rate of ECAR due to **glycolysis** (Figure 3b) was observed in those cells incubated with PA-containing media.

**Glycolytic capacity** showed significantly decreased rates in cells incubated with PA, OL and the PA/OL 1:2 ratio ( $p=0.007$ ,  $0.010$ ,  $0.005$ , respectively) (Figure 3c), while the **glycolytic reserve** (Figure 3d) only showed significant reductions in cells incubated with PA ( $p=0.044$ ) and OL ( $p=0.015$ ), compared with the basal condition.

As a complementary analysis of glycolytic function, the gene expression of SLC2A3 and HK2 was quantified. The results showed that incubation with PA induced significant increases in the expression ratio of both genes ( $p=0.007$  and  $0.013$ , respectively); the expression of these genes, however, was restored to values similar to the basal condition after incubation with OL and the PA/OL 1:2 ratio (Figures 3e and 3f).

### **Cellular energy balance**

The metabolic effects observed in the previous experiments should affect cellular energy balance. To address this, the OCR and ECAR data obtained were used to estimate ATP produced by OXPHOS and glycolysis. Figure 4a shows the ATP production rates for each of the conditions. The production rate of glycolytic ATP was significantly lower in chondrocytes incubated with PA ( $p=0.022$ ) and PA/OL ( $p=0.024$ ) in relation to the basal condition. On the contrary, production rate of glycolytic ATP was significantly higher in the OL condition when compared to the PA condition ( $p=0.046$ ). The production rate of ATP from OXPHOS showed lower values in chondrocytes incubated with all of the FA test solutions in relation to the basal condition, being significantly lower in chondrocytes incubated with PA in relation to both the basal condition ( $p=0.016$ ) and OL ( $p=0.011$ ).

The production of total and mitochondrial ATP by luminescence was also quantified in those conditions that showed alterations in the estimation of ATP production described above. The results showed a significant decrease in the production of both total ATP ( $p=0.040$ ) and mitochondrial ATP ( $p=0.004$ ) (Figure 4b) in cells incubated with PA compared to basal condition. In the case of the combined PA/OL incubation, no significant differences in the both total and mitochondrial ATP were detected in relation to the basal condition, but both were significantly higher than the PA ( $p=0.011$  and  $0.004$ , respectively).

### **Evaluation of lipid accumulation**

Visualization of prepared images using phase contrast optical microscopy revealed a large accumulation of cytoplasmic structures in cells incubated with the different FA test solutions in relation to the basal condition (Supplementary figure 1). Therefore, the possible formation of LD after staining with both OilRedO (Figure 5a) and LD540 (Figure 5b) was evaluated, demonstrating an increase of these structures in FA test solution conditions that were significantly higher when cells were incubated with OL (Figure 5c).

LD are structures with a hydrophobic center formed mainly by TG. Therefore, the presence of these glycerols was subsequently quantified in cell extracts obtained after incubation with the different FA test solutions. The analysis of the obtained absorbance values allowed us to determine that TG content is significantly higher after incubation with PA, OL and PA/OL ( $p=0.042$ ,  $0.021$  and  $0.026$ , respectively) when compared with basal condition, in agreement with the results obtained from LD stains. Moreover, TG content of cells incubated with OL is significantly higher than cells incubated with PA ( $p=0.026$ ) (Figure 5d).

## **Discussion**

In recent years, the relationship between MS and OA has generated controversy. Different studies performed on knee and hip joints lose the association after adjusting for body mass index (BMI) (26). However, the metabolic alterations that define the MS are considered among the four major environmental factors that are associated with the OA pathogenesis (27). In addition, (i) studies on painful interphalangeal OA showed that MS is significantly associated with the disease, even adjusting for both age and BMI (28) and (ii) a follow-up study carried out on a high number of subjects suggests that both overweight and obesity increase the risk of incident hand OA, a joint not subjected to

mechanical overload (7). These findings suggest that there are systemic markers related to metabolic disorders that act as etiological factors of OA in a metabolic subgroup of this disease. Among these markers, increased levels of circulating FA stand out. Articular cartilage is an avascular tissue and chondrocytes are cells with a higher capacity to maintain their synthetic functions with a minimal supply of nutrients and low oxygen consumption. Although the energy needed for chondrocyte activity comes mostly from anaerobic glycolysis, these cells contain mitochondria and oxidative mitochondrial enzymes; thus, aerobic metabolism takes place, even more when glycolysis is overflowed (29). ATP resulting from mitochondrial respiration is also known to contribute significantly to the synthesis of collagen and proteoglycans of the MEC of articular cartilage (17). Alterations of glycolysis and mitochondrial pathway in chondrocytes lead to a lowered ATP production, an alteration already described in OA chondrocytes (30–32).

One of the most novel points of this work is the study of the effect of FA overload on the metabolic function of chondrocytes. Chondrocytes incubated with FA show lower basal respiration rates and the distribution of basal OCR differs according to the FA with which the chondrocytes were incubated. The OCR data showed mitochondrial dysfunction in chondrocytes treated with PA. Thus, after incubation with PA, an increase of proton leak is generated, resulting in an OCR increase, but not an increase in ATP production. Coupling efficiency is very sensitive to bioenergetics changes and is altered before any kind of mitochondrial dysfunction (33). Following the exposure of chondrocytes to PA, a lower percentage of this parameter was in evidence, that is, a decrease in the coupling quality between OXPHOS and the electronic transport chain occurs. In contrast, when incubated with OL, the slight decrease in OCR intended for the production of ATP was accompanied by a lower rate of OCR corresponding to proton leak, with a coupling efficiency similar to the baseline condition. In addition, the stimulation of the respiratory chain to its maximum capacity after administration of FCCP showed a lower maximum capacity of respiration after incubation with PA, resulting in a lower reserve respiratory capacity. This would indicate a lower capacity of chondrocytes incubated with PA to respond to an energy demand, or how close to their bioenergetic limit these cells are (33). Furthermore, it has been described that, under oxidative stress conditions, the reserve capacity is exhausted and may eventually cause cell death when the threshold of basal respiration is reached (40). All these data indicate, therefore, that PA produces mitochondrial dysfunction in chondrocytes. On the other hand, when chondrocytes were incubated with the same concentration of OL or PA/OL, no significant variations in the parameters of respiration were observed, showing that OL appears to protect chondrocytes from PA-induced mitochondrial dysfunction.

PA-induced mitochondrial dysfunction has been reported in a study where the parameters of mitochondrial respiration were analyzed with the same methodology used in our work (36). In their paper, the authors detected differences in mitochondrial function according to the type of muscle cell incubated with PA and they correlated these differences with the amount of mitochondria. In our case, however, the deficient mitochondrial metabolism following incubation of chondrocytes with PA seems to be independent of the number of mitochondria, as indirectly quantified by calculations of mtDNA copy number by qPCR.

Other studies using different cell types confirmed the mitochondrial dysfunction caused by PA and the protective effect of OL. These studies analyzed mtDNA damage (14,26), as well as the genomic analysis of mRNA expression and DNA methylation, concluding that PA exposure induces a lower expression of genes that code for respiratory chain proteins, leading to a lower activity of the OXPHOS system and, therefore, a lower ATP production (40). In this sense, the results of our study also showed a reduction in the rate of OCR intended for the production of ATP, subsequently verified by the quantification of mitochondrial ATP in chondrocytes exposed to PA. Notably, ATP production was restored when co-incubated with OL. Another effect observed in our work, after the exposure of chondrocytes to PA and not observed in co-incubation with OL, was the remarkable increase in the production of mitochondrial superoxide anion. This agrees with numerous studies that reported that the excess of saturated FA induces cellular oxidative stress, a phenomenon described in the pathogenesis of OA (13,46). These results could indicate that saturated FA, such as PA, induce a mitochondrial dysfunction that would lead to an increase in mitochondrial reactive oxygen species, thus favoring apoptosis and inflammation in chondrocytes, a finding previously observed by Alvarez-García and co-workers.(13).

Studies carried out in other cell types showed alterations in the glycolytic pathway after incubation with PA, including decreases in the expression of glycolytic proteins and the glycolysis regulator 6-phosphofructokinase, or glycolytic activity (43,44). In our study, the ECAR data from the glycolytic analysis showed a lower glycolytic rate after incubation with PA. These observations are in agreement with the studies cited above. In our work, the cellular response when the OXPHOS pathway was inhibited showed interesting differences depending on the FA added. In the basal condition, there was an increase in ECAR corresponding to an increase in the glycolytic rate to compensate for the inhibition of the mitochondrial pathway. However, when cells were incubated with FA, the ECAR values showed low glycolytic capacity and a low glycolytic reserve. In the presence of PA, a low rate of ATP production was described throughout the glycolytic pathway. This data, in addition to the low rate of ATP production by OXPHOS, caused a decrease of total ATP production after incubation with PA. Interestingly, the low level of ATP was partially recovered by co-incubation with OL through the recovery of ATP production by OXPHOS.

Despite the low rate of glycolytic activity detected, the results of our study showed an increased expression of SLC2A3 and HK2 after exposure to PA. We speculate that one possible explanation could be that articular chondrocytes activate mechanisms that favor glucose uptake (SLC2A3) and its integration into the glycolytic pathway (HK2) to compensate for the cellular energy deficit observed both by the lower glycolytic contribution and by mitochondrial dysfunction. In order to confirm this, additional studies involving the ancillary routes of glucose metabolism, such as the pentose phosphate pathway, should be performed.

The results described thus far reveal harmful effects, related to cartilage degradation, on chondrocytes exposed to high levels of PA, which were partially reversed when co-incubated with OL. This protective effect of a monounsaturated FA has also been observed in cells of other peripheral tissues, reversing the effects of PA on insulin resistance, inflammation, mitochondrial dysfunction, oxidative stress and

apoptosis (15,16,45–47). One of the differences found after incubation with these FA that may explain the opposite effects between PA and OL, is the formation of LDs after exposure to OL. LDs are considered cellular organelles of lipid reserve coated with a phospholipid monolayer with multiple associated proteins, and a hydrophobic center composed primarily of TG or cholesterol esters (48). The differential toxicity between saturated FA, such as PA, and their co-incubation with a monounsaturated FA, such as OL, seems to be related to the ability of the latter to promote PA incorporation into TG (49–51). In our study, a striking increase in LDs after incubation with the three FA conditions was observed, but their presence and size was significantly higher when OL was present in the culture medium. These results are supported by the appearance of a higher intracellular TG content after incubation with OL. The difference, both in the amount of LDs and intracellular TG, observed after incubation with PA and the incorporation of OL into the culture medium, may indicate that, as described in other peripheral tissues (46,49), the monounsaturated FA can favor the incorporation of PA into TG, thus decreasing its toxic effects. Although the excessive accumulation of LDs in cells does seem to also have long-term lipotoxic effects, in the presence of an excess of FA, it seems that monounsaturated FA, such as OL, offer an initial cytoprotective effect on cells. This has been demonstrated in cells of the Chinese hamster ovary, in which, when the synthetic capacity of TG fails, OL acquires the same toxic effects as PA (49); this issue has not been addressed in our study. Studies that subject chondrocytes to a longer term exposure to OL would be necessary to assess the lipotoxic effect of the accumulation of LDs in these cells.

This study has some limitations that must be addressed. On the one hand, the use of primary human chondrocytes or cartilage explants would be an important support for the results obtained in our work. However, to carry it out, it would be necessary to perform the study including samples from subjects without OA and no associated metabolic disease, whose availability is limited. This justifies the use in our study of the human chondrocyte cell line T/C-28a2, a widely used cell line in *in vitro* studies of osteoarthritis (52). On the other hand, an important fact to consider is the possible toxic effect of FA concentrations on cells that could alter the results of tests such as those used in this study. In our case, as in studies conducted on other cell types (53,54), the viability test in chondrocytes T/C-28a2 allowed us to use clearly pathological AF concentrations in relation to normal serum levels(24,25).

In summary, a metabolic phenotype in OA is supported by the close relationship with pathologies associated with MS independent of BMI. This indicates that there are systemic factors associated with these pathologies that may promote the OA process. One of the systemic factor candidates is a high level of FA, known in the serum of different metabolic alterations, as well as in the synovial fluid of OA patients compared to healthy subjects. The proportion of FA was also different in these two groups, with saturated FA predominant in the synovial fluid of OA patients. Based on the results obtained in our study, saturated FA, such as PA, produce harmful effects, a mitochondrial dysfunction as well as alterations in glycolytic metabolism, events which can trigger OA pathology through the degradation of the MEC of articular cartilage. Importantly, these effects can be partially reversed by monounsaturated FA, such as OL.

## Conclusions

These results may help explain, at least in part, the close relationship of metabolic pathologies with OA, as well as help to elucidate some of the factors that can define a metabolic phenotype in OA. An accurate identification of this phenotype would lead to specific treatment that helps to combat metabolic disorders in these patients, preventing in turn the appearance as well as the OA evolution.

## Abbreviations

2-DG: 2-deoxyglucose; BSA: bovine serum albumin; BC: basal condition; BMI: body mass index; BSA: bovine serum albumin; DMEM: Dulbecco's modified eagle medium; ECAR: extracellular acidification rate; FA: fatty acids; FBS: fetal bovine serum; FCCP: carbonyl cyanide-p-trifluoromethoxyphenylhydrazone; LD: lipid droplet; MS: metabolic syndrome; mtDNA: mitochondrial DNA; OA: osteoarthritis; OCR: oxygen consumption ratio; OLG: oligomycin; OXPHOS: mitochondrial oxidative phosphorylation system; PA: palmitate; PA/OL: palmitate and oleate mix; PPR: proton production ratio; Rot/AntA: rotenone and antimycin A mixture; TG: triglycerides.

## Declarations

### Ethics approval and consent to participate

Not applicable

### Consent for publication

Not applicable

### Availability of data and materials

All data generated or analyzed during this study are included in this published article and its supplementary information files.

**Competing interests:** There are no competing interest.

### Funding

This work is supported by grants from Fondo de Investigación Sanitaria (CIBERCB06/01/0040-Spain, RETIC-RIER-RD16/0012/0002, PRB2-ISCIII-PT17/0019/0014, PI14/01254 and PI16/02124) integrated in the National Plan for Scientific Program, Development and Technological Innovation 2013–2016 and funded by the ISCIII-General Subdirection of Assessment and Promotion of Research-European Regional Development Fund (FEDER) "A way of making Europe". IRP is supported by Contrato Miguel Servet-II Fondo de Investigación Sanitaria (CPII17/00026). MEV-M is supported by FIS PI16/02124. MFM is supported by Centro de investigación biomédica en Red, Bioingeniería, Biomateriales y Nanomedicina (CIBER-BBN). AD-F is supported by FIS PI17/00210. AD-S is supported by grant IN606A-2018/023 from Xunta de Galicia, Spain. And PR-L is supported by through project PIE16/00054 (ISCIII).

## Authors contributions

**FJB and IR-P** contributed equally in the design and coordination of the study; both conceived the study, participated in its design and helped to draft the final version of the manuscript; **MEV-M** carried out the experiments and helped to draft the manuscript and data interpretation; **MF-M** supervised and helped to develop the experimental of mitochondrial and glycolytic function and interpretation; **EC-P** helped to carry out the chondrocytes culture. **SR-F** helped to carried out the stains and cytometry experiments, **AD-F, AD-S** and **PR-L** helped to carry out RNA isolation and real-time PCR experiments. All the authors approved the final version of the manuscript.

## Acknowledgements

## References

1. Kraus VB, Blanco FJ, Englund M, Karsdal MA, Lohmander LS. Call for standardized definitions of osteoarthritis and risk stratification for clinical trials and clinical use. Vol. 23, Osteoarthritis and Cartilage. 2015. p. 1233–41.
2. Mobasheri A, Batt M. An update on the pathophysiology of osteoarthritis. *Ann Phys Rehabil Med*. 2016 Dec;59(5–6):333–9.
3. Singh G, Miller JD, Lee FH, Pettitt D, Russell MW. Prevalence of cardiovascular disease risk factors among US adults with self-reported osteoarthritis: data from the Third National Health and Nutrition Examination Survey. *Am J Manag Care*. 2002 Oct;8(15 Suppl):S383-91.
4. Sowers M, Karvonen-Gutierrez CA, Palmieri-Smith R, Jacobson JA, Jiang Y, Ashton-Miller JA. Knee osteoarthritis in obese women with cardiometabolic clustering. *Arthritis Care Res*. 2009 Oct 15;61(10):1328–36.
5. Yoshimura N, Muraki S, Oka H, Kawaguchi H, Nakamura K, Akune T. Association of knee osteoarthritis with the accumulation of metabolic risk factors such as overweight, hypertension, dyslipidemia, and impaired glucose tolerance in Japanese men and women: The ROAD study. *J Rheumatol*. 2011 May 1;38(5):921–30.
6. Lee S, Kim TN, Kim SH, Kim YG, Lee CK, Moon HB, et al. Obesity, metabolic abnormality, and knee osteoarthritis: a cross-sectional study in Korean women. *Mod Rheumatol*. 2015;25(2):292–7.
7. Reyes C, Leyland KM, Peat G, Cooper C, Arden NK, Prieto-Alhambra D. Association Between Overweight and Obesity and Risk of Clinically Diagnosed Knee, Hip, and Hand Osteoarthritis: A Population-Based Cohort Study. *Arthritis Rheumatol*. 2016 Aug;68(8):1869–75.
8. Baylin A, Kabagambe EK, Siles X, Campos H. Adipose tissue biomarkers of fatty acid intake. *Am J Clin Nutr*. 2002 Oct 1;76(4):750–7.
9. Cusi K, Kashyap S, Gastaldelli A, Bajaj M, Cersosimo E. Effects on insulin secretion and insulin action of a 48-h reduction of plasma free fatty acids with acipimox in nondiabetic subjects genetically predisposed to type 2 diabetes. *AJP Endocrinol Metab*. 2007 Jan 30;292(6):E1775–81.

10. Blanco FJ. Osteoarthritis and atherosclerosis in joint disease". *Reumatol Clin*. 2018 Sep;14(5):251–3.
11. Ramachandra CJA, Mehta A, Wong P, Ja KPMM, Fritsche-Danielson R, Bhat R V, et al. Fatty acid metabolism driven mitochondrial bioenergetics promotes advanced developmental phenotypes in human induced pluripotent stem cell derived cardiomyocytes. *Int J Cardiol*. 2018 Dec 1;272:288–97.
12. Law BA, Liao X, Moore KS, Southard A, Roddy P, Ji R, et al. Lipotoxic very-long-chain ceramides cause mitochondrial dysfunction, oxidative stress, and cell death in cardiomyocytes. *FASEB J*. 2018 Mar;32(3):1403–16.
13. Alvarez-Garcia O, Rogers NH, Smith RG, Lotz MK. Palmitate has proapoptotic and proinflammatory effects on articular cartilage and synergizes with interleukin-1. *Arthritis Rheumatol*. 2014;66(7):1779–88.
14. Mei S, Ni H-M, Manley S, Bockus A, Kassel KM, Luyendyk JP, et al. Differential roles of unsaturated and saturated fatty acids on autophagy and apoptosis in hepatocytes. *J Pharmacol Exp Ther*. 2011 Nov;339(2):487–98.
15. Gao D, Griffiths HR, Bailey CJ. Oleate protects against palmitate-induced insulin resistance in L6 myotubes. *Br J Nutr*. 2009 Dec 22;102(11):1557–63.
16. Yuzefovych L, Wilson G, Rachek L. Different effects of oleate vs. palmitate on mitochondrial function, apoptosis, and insulin signaling in L6 skeletal muscle cells: role of oxidative stress. *Am J Physiol Endocrinol Metab*. 2010 Dec;299(6):E1096-105.
17. Blanco FJ, López-Armada MJ, Maneiro E. Mitochondrial dysfunction in osteoarthritis. *Mitochondrion*. 2004 Sep;4(5-6 SPEC. ISS.):715–28.
18. Blanco FJ, Rego I, Ruiz-Romero C. The role of mitochondria in osteoarthritis. Vol. 7, *Nature Reviews Rheumatology*. 2011. p. 161–9.
19. Vaamonde-García C, Riveiro-Naveira RR, Valcárcel-Ares MN, Hermida-Carballo L, Blanco FJ, López-Armada MJ. Mitochondrial dysfunction increases inflammatory responsiveness to cytokines in normal human chondrocytes. *Arthritis Rheum*. 2012 Sep;64(9):2927–36.
20. Cillero-Pastor B, Eijkel G, Kiss A, Blanco FJ, Heeren RMAA. Time-of-flight secondary ion mass spectrometry-based molecular distribution distinguishing healthy and osteoarthritic human cartilage. *Anal Chem*. 2012 Oct 11;84(21):8909–16.
21. Cousin SP, Hügl SR, Wrede CE, Kajio H, Myers MG, Rhodes CJ. Free fatty acid-induced inhibition of glucose and insulin-like growth factor I-induced deoxyribonucleic acid synthesis in the pancreatic  $\beta$ -cell line INS-1. *Endocrinology*. 2001 Jan;142(1):229–40.
22. Wu H, Ying M, Hu X. Lactic acidosis switches cancer cells from aerobic glycolysis back to dominant oxidative phosphorylation. *Oncotarget*. 2014;7(26):36–8.
23. Fernández-Moreno M, Hermida-Gómez T, Gallardo ME, Dalmao-Fernández A, Rego-Pérez I, Garesse R, et al. Generating rho-0 cells using mesenchymal stem cell lines. Dettman RW, editor. *PLoS One*. 2016 Oct 20;11(10):e0164199.
24. Joosten MM, Balvers MG, Verhoeckx KC, Hendriks HF, Witkamp RF. Plasma anandamide and other N-acylethanolamines are correlated with their corresponding free fatty acid levels under both fasting

- and non-fasting conditions in women. *Nutr Metab*. 2010 Jun 14;7(1):49.
25. Zhang J, Zhao Y, Xu C, Hong Y, Lu H, Wu J, et al. Association between serum free fatty acid levels and nonalcoholic fatty liver disease: A cross-sectional study. *Sci Rep*. 2014 Jul 25;4:5832.
  26. Felson DT, Anderson JJ, Naimark A, Walker AM, Meenan RF. Obesity and knee osteoarthritis. The Framingham Study. *Ann Intern Med* [Internet]. 1988 Jul 1 [cited 2016 Nov 22];109(1):18–24. Available from: <http://www.ncbi.nlm.nih.gov/pubmed/3377350>
  27. Berenbaum F, Wallace IJ, Lieberman DE, Felson DT. Modern-day environmental factors in the pathogenesis of osteoarthritis. *Nat Rev Rheumatol*. 2018 Nov 12;14(11):674–81.
  28. Sanchez-Santos MT, Judge A, Gulati M, Spector TD, Hart DJ, Newton JL, et al. Association of metabolic syndrome with knee and hand osteoarthritis: A community-based study of women. *Semin Arthritis Rheum*. 2019 Apr;48(5):791–8.
  29. Spencer CA, Palmer TN, Mason RM. Intermediary metabolism in the Swarm rat chondrosarcoma chondrocyte. *Biochem J*. 1990 Feb 1;265(3):911–4.
  30. Rego-perez I, Fernandez-moreno M, Soto-hermida A, Fenandez-lopez C, Oreiro N, Blanco FJ. Mitochondrial genetics and osteoarthritis. *Front Biosci (Schol Ed)*. 2013 Jan 1;5:360–8.
  31. Maneiro E, Martín MA, De Andres MC, López-Armada MJ, Fernández-Sueiro JL, Del Hoyo P, et al. Mitochondrial respiratory activity is altered in osteoarthritic human articular chondrocytes. *Arthritis Rheum*. 2003;48(3):700–8.
  32. Ruiz-Romero C, Carreira V, Rego I, Remeseiro S, López-Armada MJ, Blanco FJ. Proteomic analysis of human osteoarthritic chondrocytes reveals protein changes in stress and glycolysis. *Proteomics*. 2008 Feb;8(3):495–507.
  33. Brand M, Nicholls D. Brand MD, Nicholls DG Assessing mitochondrial dysfunction in cells. *Biochem J* 435:297-312. *Biochem J*. 2011;312(April):297–312.
  34. Dranka BP, Hill BG, Darley-Usmar VM. Mitochondrial reserve capacity in endothelial cells: The impact of nitric oxide and reactive oxygen species. *Free Radic Biol Med*. 2010;48(7):905–14.
  35. Dranka BP, Benavides GA, Diers AR, Giordano S, Zelickson BR, Reily C, et al. Assessing bioenergetic function in response to oxidative stress by metabolic profiling. *Free Radic Biol Med*. 2011;51(9):1621–35.
  36. Patková J, Anděl M, Trnka J. Palmitate-induced cell death and mitochondrial respiratory dysfunction in myoblasts are not prevented by mitochondria-targeted antioxidants. *Cell Physiol Biochem*. 2014 May 5;33(5):1439–51.
  37. Egnatchik RA, Leamy AK, Noguchi Y, Shiota M, Young JD. Palmitate-induced activation of mitochondrial metabolism promotes oxidative stress and apoptosis in H4IIEC3 rat hepatocytes. *Metabolism*. 2014 Feb;63(2):283–95.
  38. Rachek LI, Musiyenko SI, LeDoux SP, Wilson GL. Palmitate induced mitochondrial deoxyribonucleic acid damage and apoptosis in L6 rat skeletal muscle cells. *Endocrinology*. 2007 Jan;148(1):293–9.

39. Hirabara SM, Curi R, Maechler P. Saturated fatty acid-induced insulin resistance is associated with mitochondrial dysfunction in skeletal muscle cells. *J Cell Physiol.* 2010 Jan;222(1):187–94.
40. Hall E, Volkov P, Dayeh T, Bacos K, Ronn T, Nitert MD, et al. Effects of palmitate on genome-wide mRNA expression and DNA methylation patterns in human pancreatic islets. *BMC Med.* 2014 Jun 23;12(1):103.
41. Lambertucci RH, Hirabara SM, Silveira L dos R, Levada-Pires AC, Curi R, Pithon-Curi TC. Palmitate increases superoxide production through mitochondrial electron transport chain and NADPH oxidase activity in skeletal muscle cells. *J Cell Physiol.* 2008 Sep;216(3):796–804.
42. Lee E, Choi J, Lee HS. Palmitate induces mitochondrial superoxide generation and activates AMPK in podocytes. *J Cell Physiol.* 2017 Feb 18;232(12):3209–17.
43. Botchlett R, Li H, Guo X, Qi T, Zhao JJ, Zheng J, et al. Glucose and Palmitate Differentially Regulate PFKFB3/iPKF2 and Inflammatory Responses in Mouse Intestinal Epithelial Cells. *Sci Rep.* 2016 Sep 8;6(1):28963.
44. Hovsepyan M, Sargsyan E, Bergsten P. Palmitate-induced changes in protein expression of insulin secreting INS-1E cells. *J Proteomics.* 2010 Apr 18;73(6):1148–55.
45. Kadotani A, Tsuchiya Y, Hatakeyama H, Katagiri H, Kanzaki M. Different impacts of saturated and unsaturated free fatty acids on COX-2 expression in C 2 C 12 myotubes. *Am J Physiol Metab.* 2009 Dec 1;297(6):E1291–303.
46. Ricchi M, Odoardi MR, Carulli L, Anzivino C, Ballestri S, Pinetti A, et al. Differential effect of oleic and palmitic acid on lipid accumulation and apoptosis in cultured hepatocytes. *J Gastroenterol Hepatol.* 2009 May;24(5):830–40.
47. Coll T, Eyre E, Rodríguez-Calvo R, Palomer X, Sánchez RM, Merlos M, et al. Oleate reverses palmitate-induced insulin resistance and inflammation in skeletal muscle cells. *J Biol Chem.* 2008;283(17):11107–16.
48. Horton M, Read JC, Fitton D, Toth N, Little L. Too cool at school - Understanding cool teenagers. *PsychNology J.* 2012;10(2):73–91.
49. Listenberger LL, Han X, Lewis SE, Cases S, Farese R V, Ory DS, et al. Triglyceride accumulation protects against fatty acid-induced lipotoxicity. *Proc Natl Acad Sci U S A.* 2003 Mar 18;100(6):3077–82.
50. Cnop M, Hannaert JC, Hoorens A, Eizirik DL, Pipeleers DG. Inverse Relationship between Cytotoxicity of Free Fatty Acids in Pancreatic Islet Cells and Cellular Triglyceride Accumulation. *Diabetes.* 2001;50(8):1771–7.
51. Gillet C, Spruyt D, Rigutto S, Dalla Valle A, Berlier J, Louis C, et al. Oleate abrogates palmitate-induced lipotoxicity and proinflammatory response in human bone marrow-derived mesenchymal stem cells and osteoblastic cells. *Endocrinology.* 2015 Nov;156(11):4081–93.
52. Nogueira-Recalde U, Lorenzo-Gómez I, Blanco FJ, Loza MI, Grassi D, Shirinsky V, et al. Fibrates as drugs with senolytic and autophagic activity for osteoarthritis therapy. *EBioMedicine.* 2019 Jul;45:588–605.

53. Abu Bakar MH, Sarmidi MR, Tan JS, Mohamad Rosdi MN. Celastrol attenuates mitochondrial dysfunction and inflammation in palmitate-mediated insulin resistance in C3A hepatocytes. *Eur J Pharmacol.* 2017 Mar 15;799:73–83.
54. Chen X, Yi L, Song S, Wang L, Liang Q, Wang Y, et al. Puerarin attenuates palmitate-induced mitochondrial dysfunction, impaired mitophagy and inflammation in L6 myotubes. *Life Sci.* 2018 Aug 1;206:84–92.

## Additional File Legends

**Additional file 1. Table S1 (.docx).** UPL primers and probes of the analyzed genes grouped

by their function

**Additional file 2. Table S2 (.docx).** Parameters calculated to assess mitochondrial function from the oxygen consumption rate (OCR) **(a)** and glycolytic function from the extracellular acidification rate (ECAR) **(b)**

**Additional file 3. Figure S1 (.tiff).** Representative images of the structural changes detected in chondrocytes by phase contrast optical microscopy (200x). BC:basal condition; PA: palmitic acid; OL:oleic acid.

## Figures

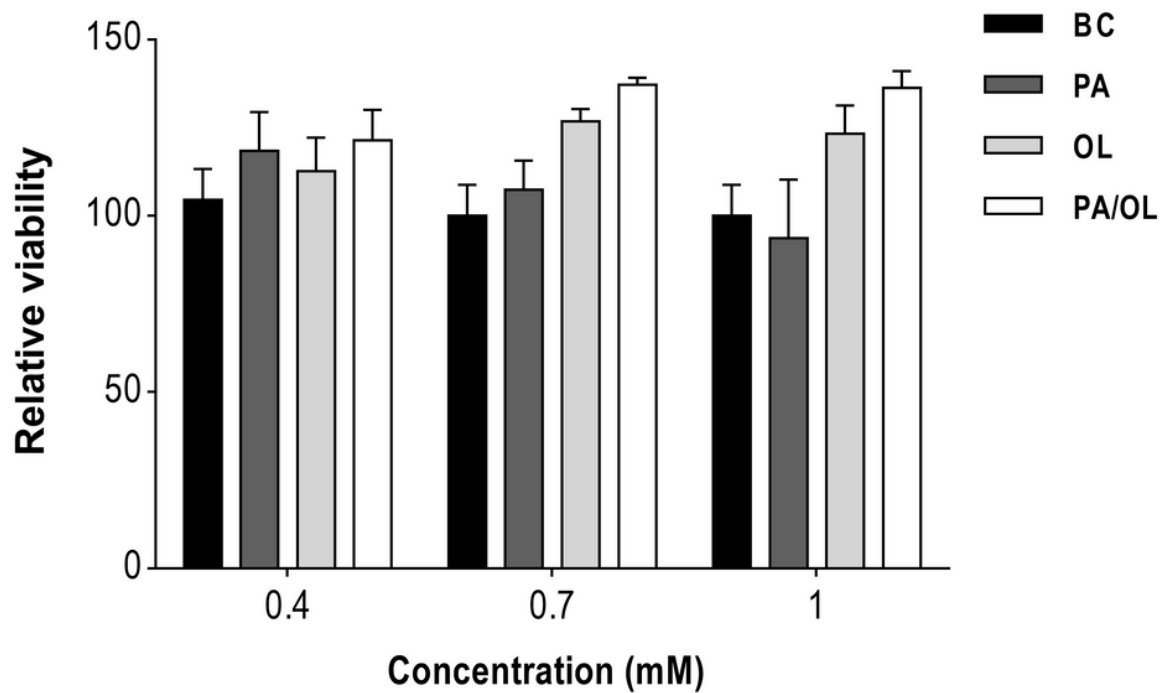


**Figure 1**

Quantification of the effects of fatty acid concentrations on cell viability. The values, expressed in relation to the baseline condition (BC) to which 100% is awarded, correspond to the mean value  $\pm$  deviation standard.

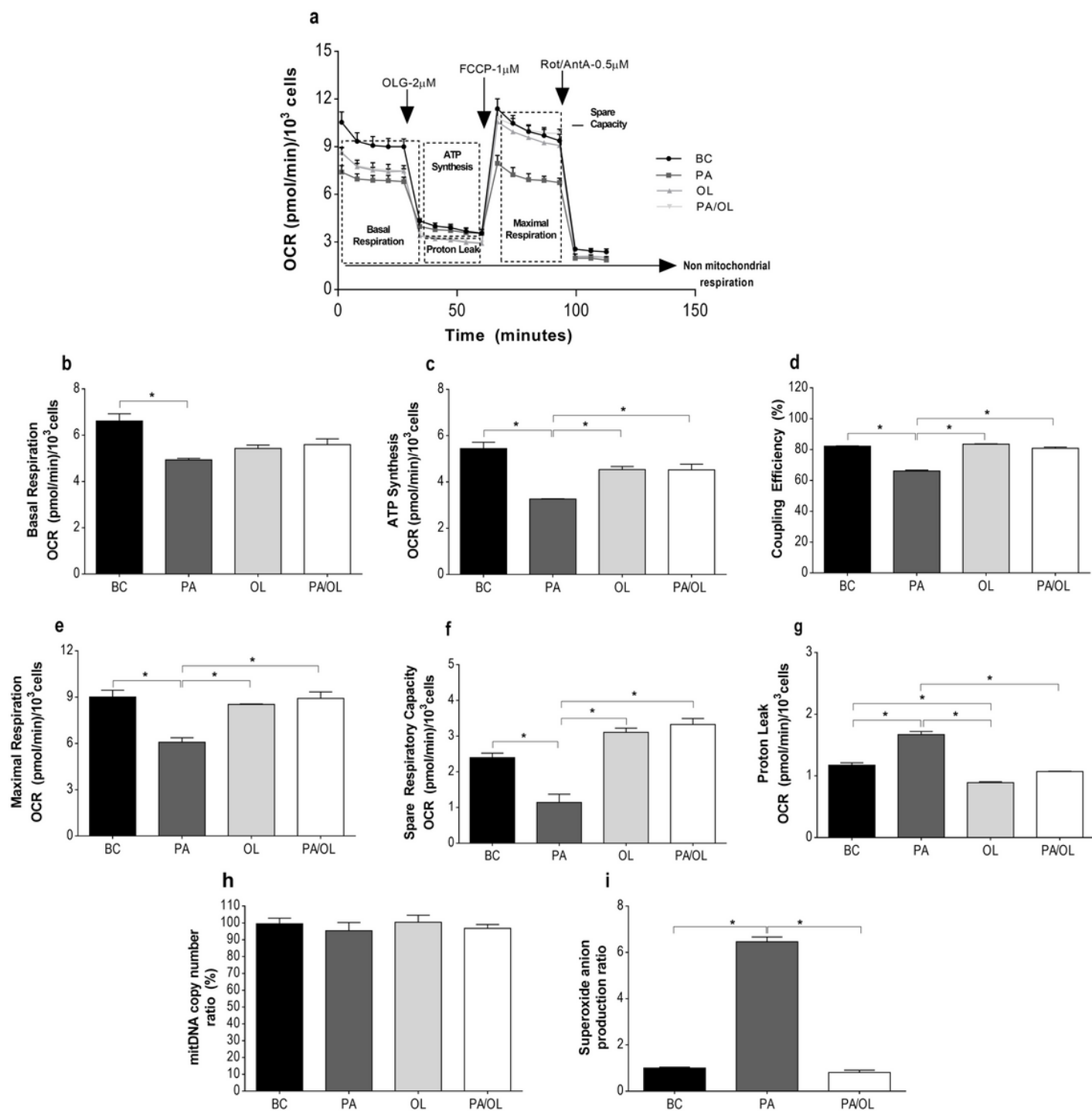


**Figure 2**

analysis of mitochondrial function by measurement of the oxygen consumption rate (OCR). (a) Representation of the OCR versus time for each of the fatty acid (FA) test solution incubations following the successive addition of each of the modulators of mitochondrial activity: OLG at 2 $\mu$ M; FCCP at 1 $\mu$ M and a mixture of Rot/AntA at 0.5 $\mu$ M. From these OCR values, the following parameters were calculated: (b) OCR due to basal respiration; (c) ATP synthesis; (d) coupling efficiency (%); (e) maximal respiration; (f) spare respiratory capacity ; (g) proton leak; (h) percentage (%), relative to the basal condition, of the

number of copies of mitochondrial DNA; and (i) ratio in relation to BC of mitochondrial superoxide anion quantification expression. The mean value  $\pm$  standard deviation is represented in each case; \*,  $p < 0.05$ . BC = basal condition; PA=palmitic acid; OL=oleic acid; OLG =oligomycin; FCCP=carbonyl cyanide-p-trifluoromethoxyphenylhydrazone; ROT=rotenone; AntA =antimycin A.

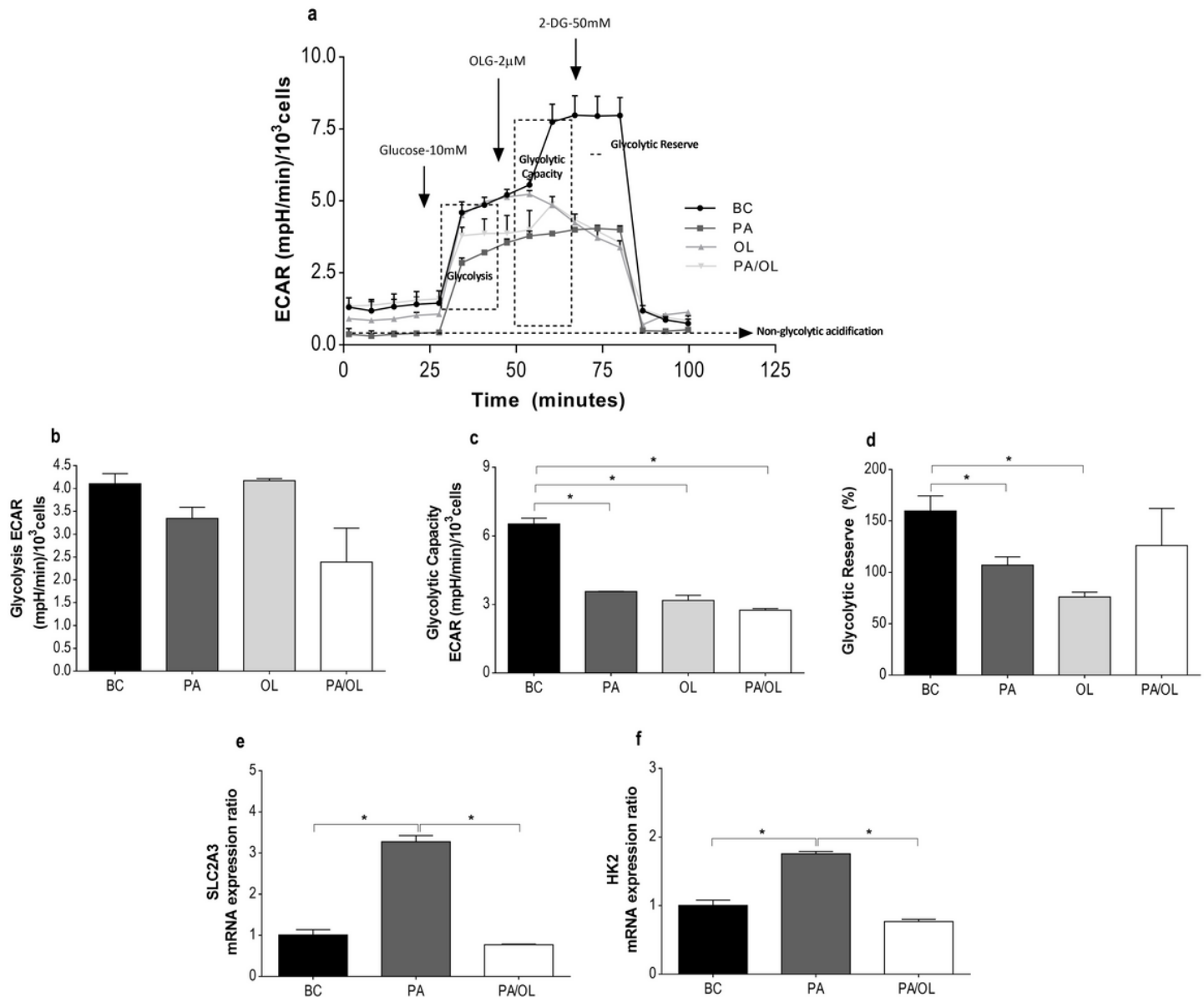


**Figure 3**

Analysis of glycolytic function by measurement of the rate of extracellular acidification (ECAR). (a) Representation of the ECAR versus time for each of the fatty acid (FA) test solution incubations following

the addition of glucose at 10mM, OLG at 2 $\mu$ M and 2-DG at 50 $\mu$ M. From these ECAR values, the following parameters were calculated: (b) ECAR due to glycolysis; (c) the glycolysis capacity; and (d) the glycolytic reserve (%). Gene expression ratios of (e) SLC2A3 and (f) HK2 after FA incubations are also represented in relation to the BC. The mean value  $\pm$  standard deviation is represented in each case; \*,  $p < 0.05$ . BC = basal condition; PA=palmitic acid; OL=oleic acid; OLG = oligomycin; 2-DG = 2 deoxyglucose

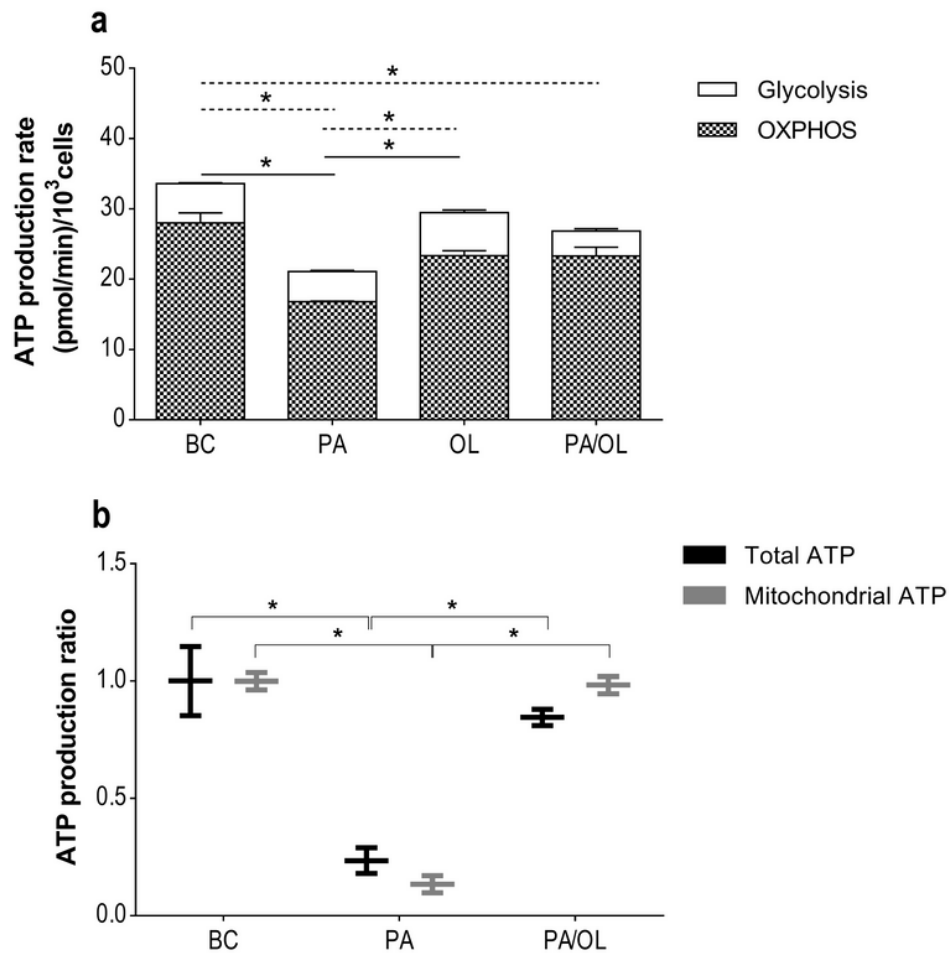
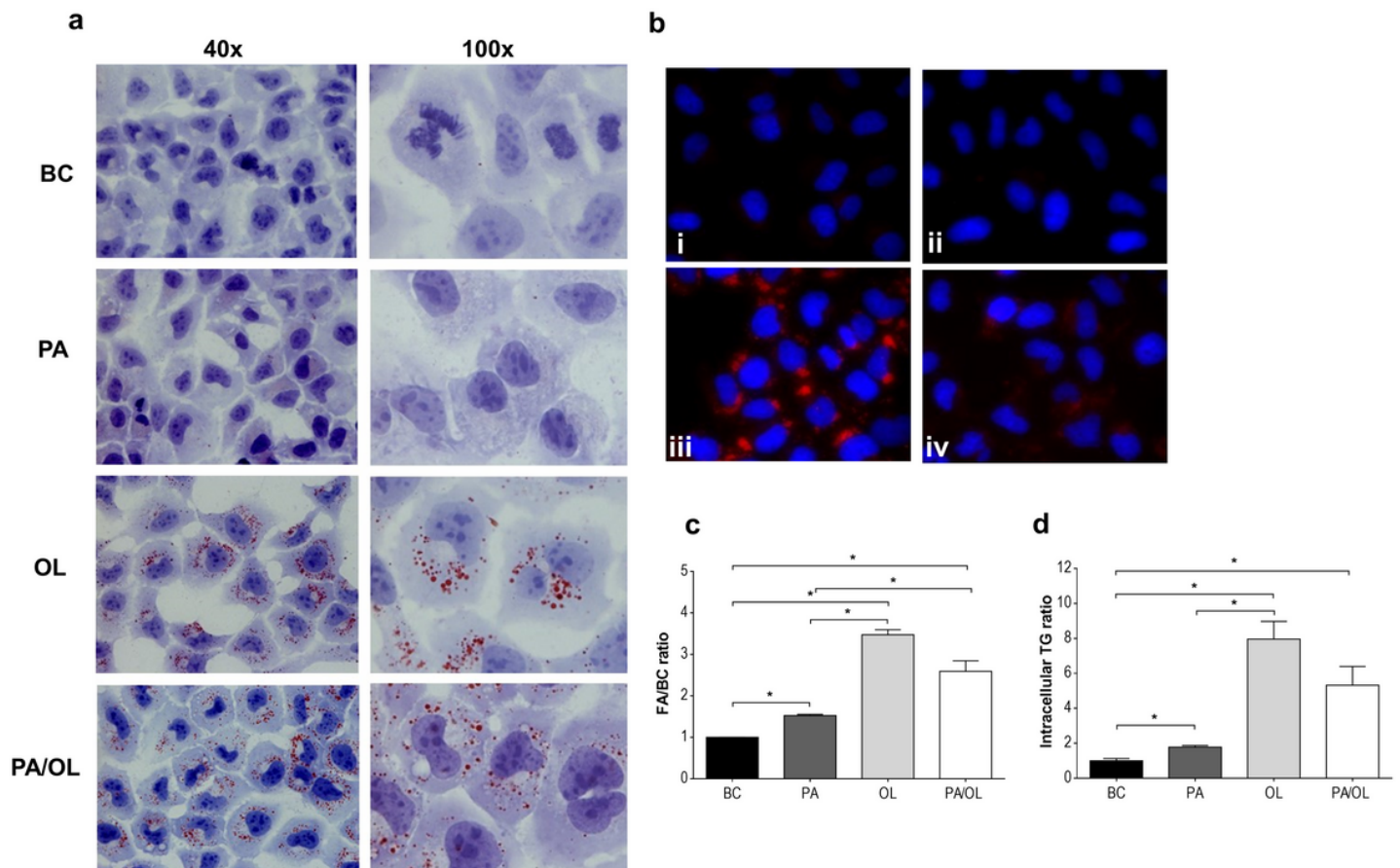


Figure 4

Evaluation of energy balance. (a) Total ATP production rate estimated from the values of oxygen consumption (OCR) and the proton production rate (PPR). The production rate of total ATP in pmol/min and the distribution of the rate corresponding to the production by OXPHOS (stripes) and by the glycolytic pathway (white) is represented. Significant differences ( $p < 0.05$ ) are represented by continuous line (OXPHOS) and discontinuous line (glycolytic pathway). (b) Measurement of ATP production by luminescence, including both total and mitochondrial ATP. The data are represented as the mean of the ratio in relation to the  $BC \pm$  standard deviation. \*,  $p < 0.05$ . BC = basal condition; PA=palmitic acid; OL=oleic acid; OXPHOS = oxidative phosphorylation



**Figure 5**

Analysis of lipid droplet formation. (a) Images (400x) obtained by optical microscopy with Oil Red O dye and (b) by fluorescence microscopy with the LD540 stain, following incubations with the following fatty acid (FA) test solutions: (i) BC, (ii) PA, (iii) OL, and (iv) PA/OL. (c) Quantification by flow cytometry of the LD540 signal. (d) Triglyceride intracellular levels. In each case, the data are represented as the mean of the ratio in relation to the  $BC \pm$  standard deviation. \*  $p < 0.05$ . BC = basal condition; PA=palmitic acid; OL=oleic acid; TG = triglyceride

## Supplementary Files

This is a list of supplementary files associated with this preprint. Click to download.

- [Additionalfile1.TableS1.docx](#)
- [Additionalfile2.TableS2.docx](#)
- [Additionalfile3.FigureS1.tif](#)